Appendix

Title: Plk1 protects kinetochore-centromere architecture against microtubule pulling forces

Authors:
Robert F. Lera[1,2]
Roshan X. Norman[1,2,†]
Marie Dumont[3,†]
Alexandra Dennee[1,2]
Joanne Martin-Koob[1,2]
Daniele Fachinetti[3]
Mark E. Burkard[1,2,*]

Author Affiliations:
[1] Department of Medicine, Division of Hematology/Oncology, School of Medicine and Public Health, University of Wisconsin, Madison, WI, USA

[2] UW Carbone Cancer Center, University of Wisconsin, Madison, WI, USA

[3] Institut Curie, PSL Research University, CNRS, UMR 144, 26 rue d'Ulm, 75005 Paris, France.

***Corresponding author:**
Mark E. Burkard, 1111 Highland Avenue, WIMR 6059, Madison WI, UW 53705
Phone: 608-262-2803, email: mburkard@wisc.edu

[†] These authors contributed equally to this work

Table of Contents

Materials and Methods

Cell Culture and Cell Line Derivation

EGFP-Plk1^{as} cells stably expressing mCherry-H2B were derived as previously reported [1]

SNAP labeling of CENPA-SNAP-3xFlag RPE1 cells was performed as illustrated (**Appendix Figure S3**). Briefly, existing CENPA-SNAP was blocked with SNAP-Cell Block (NEB) diluted in cell culture media for 30 min, rinsed 2x with HBSS, then replenished with fresh media. CENPA-SNAP was labeled with SNAP-Cell 505 STAR (NEB), diluted in cell culture media for 30 min, rinsed 2x with fresh media, then replenished with fresh media. Please refer to **Appendix Table S2** for working concentrations.

Live-cell microscopy

RPE1 cells stably expressing EGFP-Plk1^{as} and mCherry-H2B were seeded at low density in 6-well optical bottom plates (MatTek) and challenged with chemicals and imaged as indicated in **Appendix Figure S1.**

Image acquisition was performed on a Nikon Eclipse Ti inverted microscope equipped with motorized stage (Prior Scientific), environmentally maintained at 37°C and 5% CO_2 (InVivo Scientific), Lumen200PRO epifluorescence light source (Prior Scientific), 20x/0.5NA ELWD (Plan Fluor) objective, and CoolSNAP HQ2 CCD camera (Photometrics). Brightfield and mCherry images were acquired every 4 minutes throughout filming.

Results are the combination of 2 independent experiments.

Immunoblotting

Cells were challenged with 0.2 μg/ml nocodazole for 19 h, pelleted, frozen down and stored at -80°C prior to use. Cell pellets were lysed in buffer (50 mM HEPES pH 7.5, 100 mM NaCl, 0.5% NP-40, 10% glycerol) containing phosphatase inhibitors (10 mM sodium pyrophosphate, 5 mM β-glycerolphosphate, 50 mM NaF, 0.3 mM Na_3VO_4), 1mM PMSF, 1x protease inhibitor cocktail (Thermo-Scientific) and 1 mM dithiothreitol. Proteins were separated by SDS-PAGE, transferred to Immobilon PVDF membrane (Millipore), and blocked for 30 min in 4% milk and 0.1% Tween-20 Tris buffered saline ph 7.4 (TBST+milk). Membranes were incubated with gentle agitation overnight at 4°C with primary antibodies (**Apppendix Table S2**) diluted in TBST+milk, washed 3x with TBST, incubated for 1 h at room temperature in secondary antibodies conjugated to horse radish peroxidase diluted 1:10,000 in TBST+milk.

Membranes were washed and developed with luminol/peroxide (Millipore) and visualized with a ChemiDoc MP imaging system, controlled by Image Lab 4.1 (Bio Rad). All results were obtained from single gels. To simultaneously probe for the protein of interest and the loading marker, the membrane was divided in two after transfer and incubated in separate antibody solutions.

Appendix Tables

Appendix Table S1. List of primers used in study

NAME	SEQUENCE
YFP FWD	5'-ATGGTGAGCAAGGGCGAG-3'
CENPA REV (+STOP)	5'-TCAGCCGAGTCCCTCCTCA-3'
CENPB FWD	5'-ATGGGCCCCAAGAGGC-3'
CENPB(1-158) REV (+STOP)	5'-TCAGGCCGGACTGGCAGGC-3'
CENPA FWD	5'-GGAGACAUATGGGCCCGCGCCG-3'
CENPA REV (+STOP)	5'-GGGAAAGUTCAGCCGAGTCCCTCCTCAAGG-3'
CENPB FWD	5'-GGAGACAUATGGGCCCCAAGAGGCG-3'
CENPB REV (+STOP)	5'-GGGAAAGUTCAGCTTTGATGTCCAAGACCTC-3'
INCENP FWD	5'-ATGGGGACGACGGCCCCAGGGC-3'
INCENP REV (+STOP)	5'-TCATCTCTTCTTCCGTCGGTTCTTC-3'
XIX-NotI-CENPA FWD	5'-TTGGAACGCTGCAGGAATTGATCCGCGGCCGCATGGGCCCGCGCC-3'
SNAP-AgeI-CENPA REV	5'AGTCTTTGTCCATACCGGTGCCGAGTCCCTCCTCAAGG-3'
CENPA-AgeI-SNAP FWD	5'-AGGGACTCGGCACCGGTATGGACAAAGACTGCGAAATGAAGC-3'
Flag-XbaI-SNAP REV	5'-ATCACCGTCATGGTCTTTGTAGTCTCTAGAACCCAGCCCAGGCTTG-3'
3x-Flag G-BLOCK TOP	5'-GGGCAAGCCTGGGCTGGGTTCTAGAGACTACAAAGACCATGACGGTGATTATAAAGATCATGATATCGATTACAAGGATGACGATGACAAGTAAACCGGTAGGCCTCGTACGCTTAATTAACGGA-3'
3x-Flag G-BLOCK BOTTOM	5'-TCCGTTAATTAAGCGTACGAGGCCTACCGGTTTACTTGTCATCGTCATCCTTGTAATCGATATCATGATCTTTATAATCACCGTCATGGTCTTTGTAGTCTCTAGAACCCAGCCCAGGCTTGCCC-3'

Appendix Table S2. List of antibodies/dyes used in study

Antibody/Dye	Source	Dilution / Working conc.
Human anti-ACA	Immunovision (HCT-0100)	1:1000 (IF)
	Holzel diagnostika (15-235-0001)	1:500 (IF, Fig 5a)
Goat anti-BLM (C-18)	Santa Cruz Biotechnology (sc-7790)	1:250 (IF)
Sheep anti-BubR1	Stephen Taylor (Taylor, J Cell Sci, 2001) [2]	1:500 (IF)
Mouse anti-CENPA (3-19)	Abcam (ab13939)	1:250-1:500 (IF)
Rabbit anti-CENPB	Millipore (07-735)	1:100 (IF)
Rabbit anti-CENP-C	Iain Cheeseman (Gascoigne & Cheeseman, 2011) [3]	1:1000 (IF)
Guinea pig anti-CENP-C	MBL (PD030)	1:1000 (IF, Fig 5)
Rabbit anti-CENP-T	Iain Cheeseman (Gascoigne & Cheeseman, 2011) [3]	1:1000 (IF)
DAPI	Sigma-Aldrich (D9542)	1 μg/ml (IF)
Mouse anti-Flag (M2)	Sigma-Aldrich (F1804)	1:500 (IF)
Mouse anti-Flag (M2) HRP	Sigma-Aldrich (A8592)	1:20,000 (WB)
Rabbit anti-GAPDH	Cell Signaling (14C10)	1:1000 (WB)
Mouse anti-Hec1 (9G3)	Abcam (ab3613)	1:1000 (IF)
Mouse anti-phosphoH3-S10 (6G3)	Cell Signaling (9706)	1:100 (IF)
Rabbit anti-Knl1(CASC5)	Bethyl laboratories (A300-805A)	1:500 (IF)
Rabbit anti-Mad1	Beth Weaver (Ryan et al, 2012) [4]	1:2000 (IF)

Mouse anti-Nuf2 (28-37)	Upstate (05-905)	1:100 (IF)
Mouse anti-PICH/ERCC6L (3F12-2B10)	Abnova (H00054821-M01)	1:500 (IF)
Rabbit anti-PICH/ERCC6L	Abnova (H00054821-D01P)	1:300 (WB)
Mouse anti-Plk1 (F8)	Santa Cruz Biotechnology (sc-17783)	1:500 (IF)
SNAP-Cell 505-STAR	New England Biolabs (S9103S)	2 μM (Fig. EV4b) 10 μM (Fig. 4)
SNAP-Cell Block	New England Biolabs (S9106S)	2 μM
SNAP-Cell TMR-STAR	New England Biolabs (S9105S)	2.4 μM
Rat anti-Tubulin (YL1/2)	EMD Millipore (MAB1864)	1:1000 (WB), 1:1000 (IF)
Rabbit anti-Vinculin	Cell Signaling (E1E9V)	1:1000 (WB)

Appendix Table S3. List of chemicals used in study

Chemical	Source	Working conc.
3-MB-PP1	Toronto Research Chemicals (A602960)	200 nM
AZ-3146	Selleck Chemicals (S2731)	2 μM
BI-2536	Selleck Chemicals (S1109)	various
Geneticin (G418 sulfate)	Gibco (11811-023)	0.4 mg/ml
monastrol	Tocris Bioscience (1305)	100 μM
MG-132	Enzo Life Sciences (BML-PI102)	10 μM
nocodazole	Sigma-Aldrich (M1404)	various
paclitaxel	Enzo Life Sciences (BML-T104)	20 nM
reversine	Cayman Chemical (10004412)	500 nM
thymidine	Calbiochem (6060)	3 mM

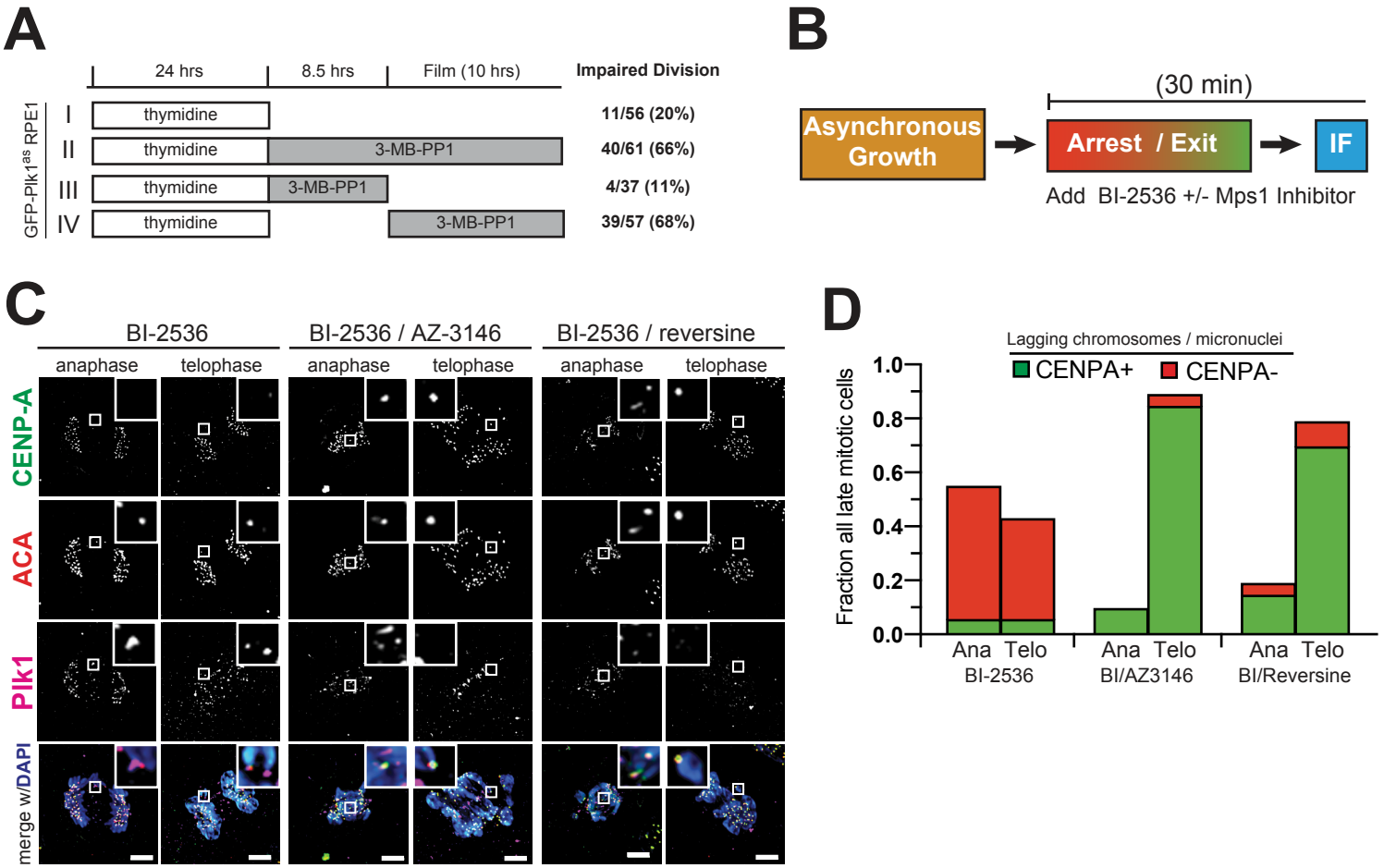

Appendix Figure S1 – Kinetochore integrity requires Plk1 activity to resist microtubule tension (related to Figure 1)

A Illustrative methodology to determine when Plk1 activity is important for chromosome segregation. mCherry-H2B-expressing EGFP-Plk1as RPE1 cells were synchronized in S-phase by thymidine block then released for 8.5 h prior to live imaging for 10 h. Plk1 was inhibited (3-MB-PP1) in early G2 (III) or late G2/M (IV) as indicated. Additional controls included no inhibition (I) or continuous inhibition (II). Values at right indicate number of anaphase cells with impaired division/total number of mitotic cells observed per condition.

B Illustrative methodology to determine if microtubule tension is required for kinetochore eviction with Plk1 inhibition. Asynchronously growing RPE1 cells were challenged for 30 min with 200 nM BI-2536 (fully inhibit Plk1 activity) and AZ3146 or reversine (force mitotic exit without full chromosome biorientation) prior to fixation and immunofluorescence analysis. Anaphase and telophase cells were identified by central spindle localized Plk1 and decondensed DNA, respectively. Note, full Plk1 inhibition with BI-2536 prevents bipolar spindle formation and collapses bipolar spindles [5], thus the analyzed cells were likely inhibited in mid-late prometaphase.

C Representative maximal-intensity projection micrographs of anaphase and telophase cells challenged as described in (B). Insets highlight the presence or absence of CENP-A at kinetochores, indicated by ACA. Scale bars, 5 μm.

D Graph shows fraction of all late mitotic cells with CENP-A localized to lagging chromosomes or micronuclei in anaphase or telophase, respectively, from (B-C). (n= 10 cells/mitotic phase from 1 experiment). Localization based on qualitative observation.

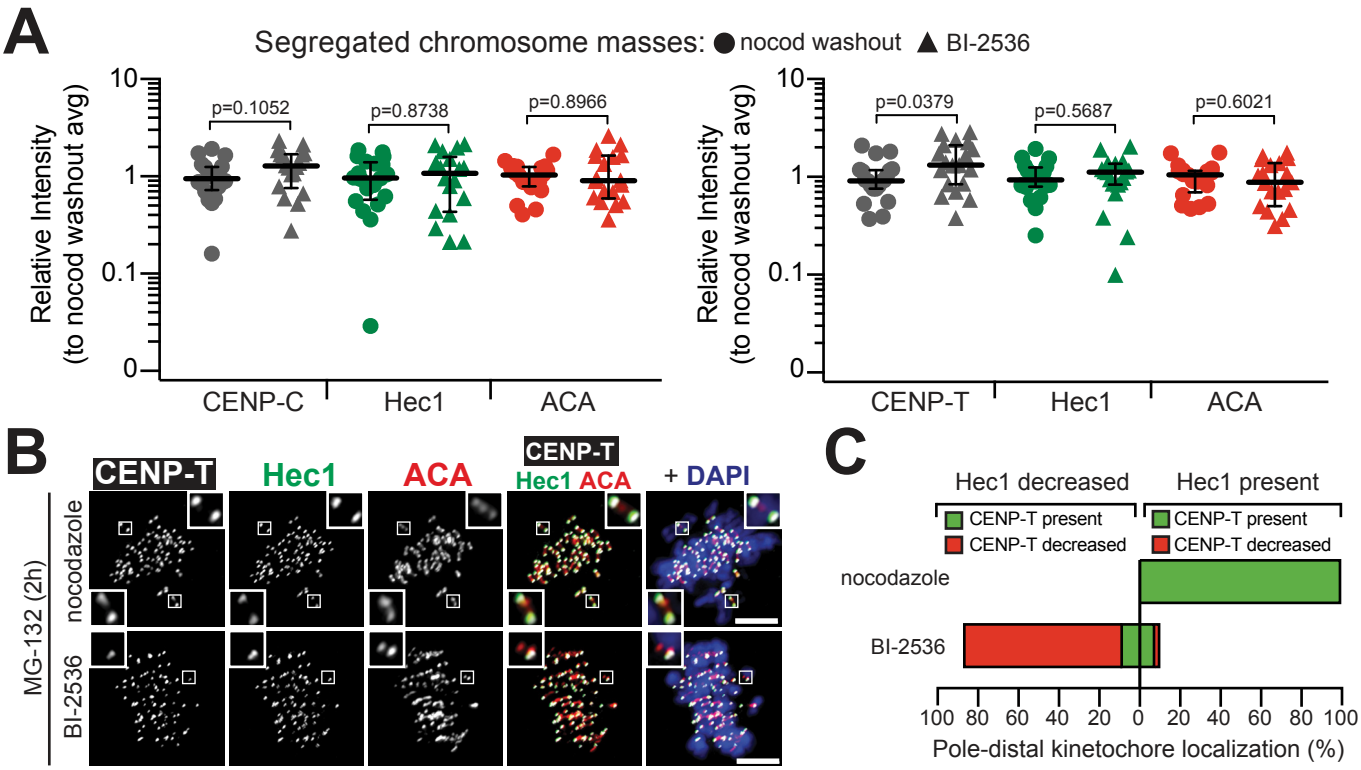

Appendix Figure S2 – The integrity defect extends to CENP-C and CENP-T (related to Figure 3)

A Graph shows relative volume intensities of CENP-C (left) or CENP-T (right), Hec1 and ACA at segregated kinetochores after Plk1 inhibition or nocodazole washout (Figure 3E). Each symbol represents all segregated kinetochores/cell (n= 10 cells/experiment; 3 independent experiments). Bars indicate median kinetochore intensity and interquartile range. Significance determined by two-tailed Mann-Whitney test.

B Representative maximal-intensity projection micrographs of metaphase cells with misaligned chromosome pairs after 2h Plk1 inhibition (BI-2536) or nocodazole challenge. Insets highlight distribution of CENP-T and Hec1 at misaligned kinetochore pairs, indicated by ACA. MG-132 was used to prevent mitotic cells from entering anaphase. Scale bars, 5 μm.

C Graph shows average percentage of misaligned pole-distal kinetochores with localized (green/lt green) or decreased (red/pink) Hec1 and CENP-T from (H). (n= 1-8 kinetochore pairs/cell; 10 cells from 1 experiment). “Decreased” intensity indicates ≤50% intensity of sister kinetochore.

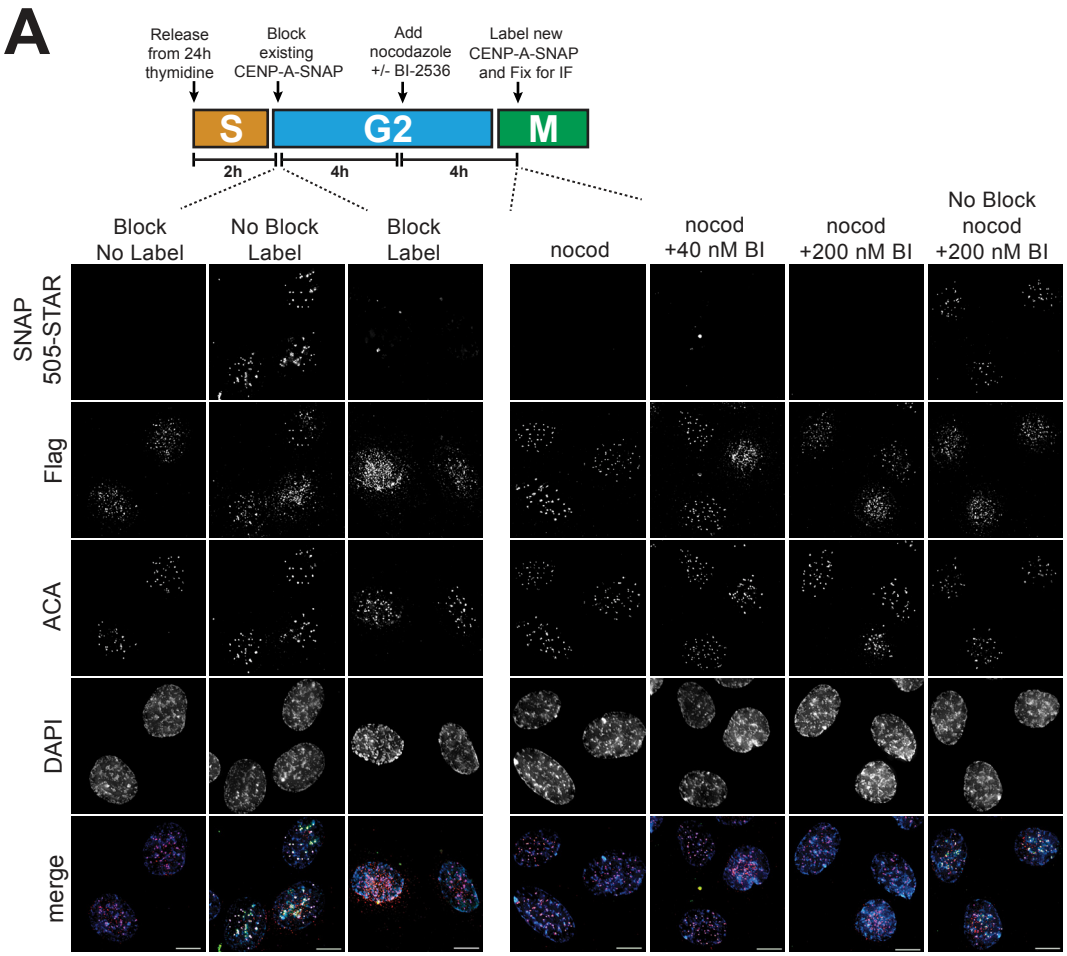

Appendix Figure S3 – Plk1 inhibition does not induce aberrant CENP-A loading (related to Figure EV4)

A Analysis of CENP-A centromere turnover during G2 in RPE1 CENPA-SNAP cells. (Top) Illustrative strategy. After release from 24 h thymidine synchronization, existing CENPA-SNAP was blocked using SNAP Cell Block. 4 h later, cells were challenged with BI-2536 (to inhibit Plk1), 200 μg/ml nocodazole (to arrest cells in mitosis), or both. 4 h later, newly synthesized CENP-A was labeled with SNAP 505-STAR. (Bottom) Representative micrographs of interphase cells indicating lack of CENP-A turnover at centromeres with or without Plk1 inhibition. Scale bars, 5 μm.

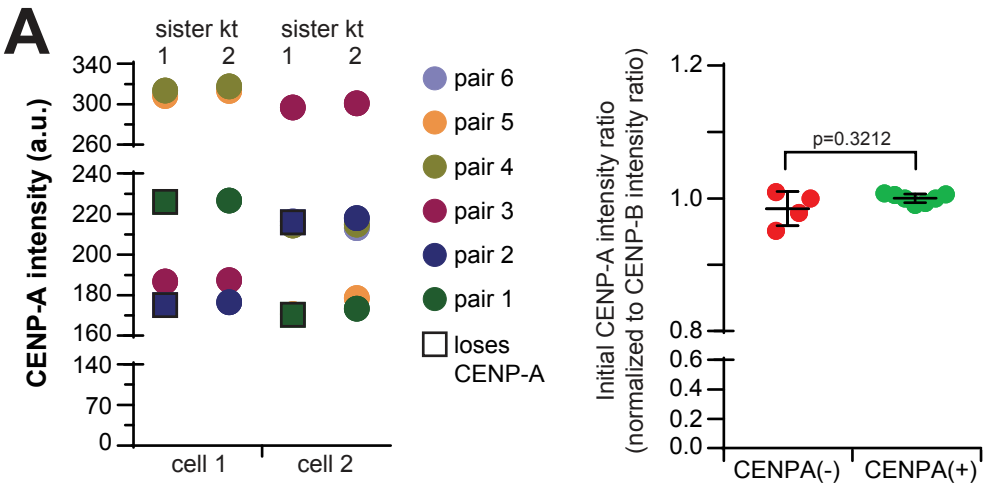

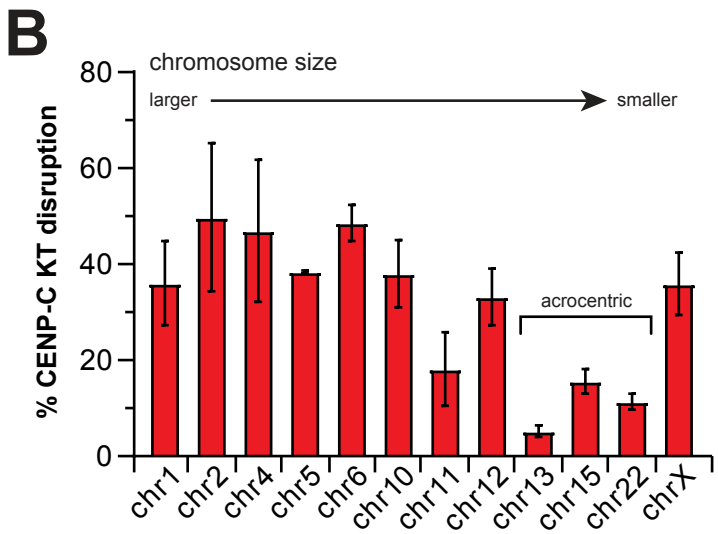

Appendix Figure S4– Intrinsic chromosome features, but not initial CENP-A levels, suggest likelihood of kinetochore rupture (related to Figure 4)

A Left, Initial CENPA volume intensities of metaphase kinetochore pairs challenged with 40 nM BI-2536. Circles represent kinetochores that retain CENP-A, whereas squares represent kinetochores that lose CENPA, becoming lagging (cell 1) or misaligned (cell 2) chromosomes. Right, Plot of the ratio of initial CENPA intensity to the corresponding CENPB intensity for the kinetochore retaining CENPA (green) and the kinetochore losing CENPA (red). Bars represent average relative intensity (± SD). Significance determined by two-tailed Mann-Whitney test.

B Graph shows frequency of CENP-C disruption occurring at specific chromosomes. Chromosomes are arranged by size, with the exception of chromosome X. Acrocentric chromosomes are also indicated. Data represents average percentage (± SEM) of kinetochores pairs exhibiting disrupted CENP-C (n= 20 chromosomes from 2 independent experiments).

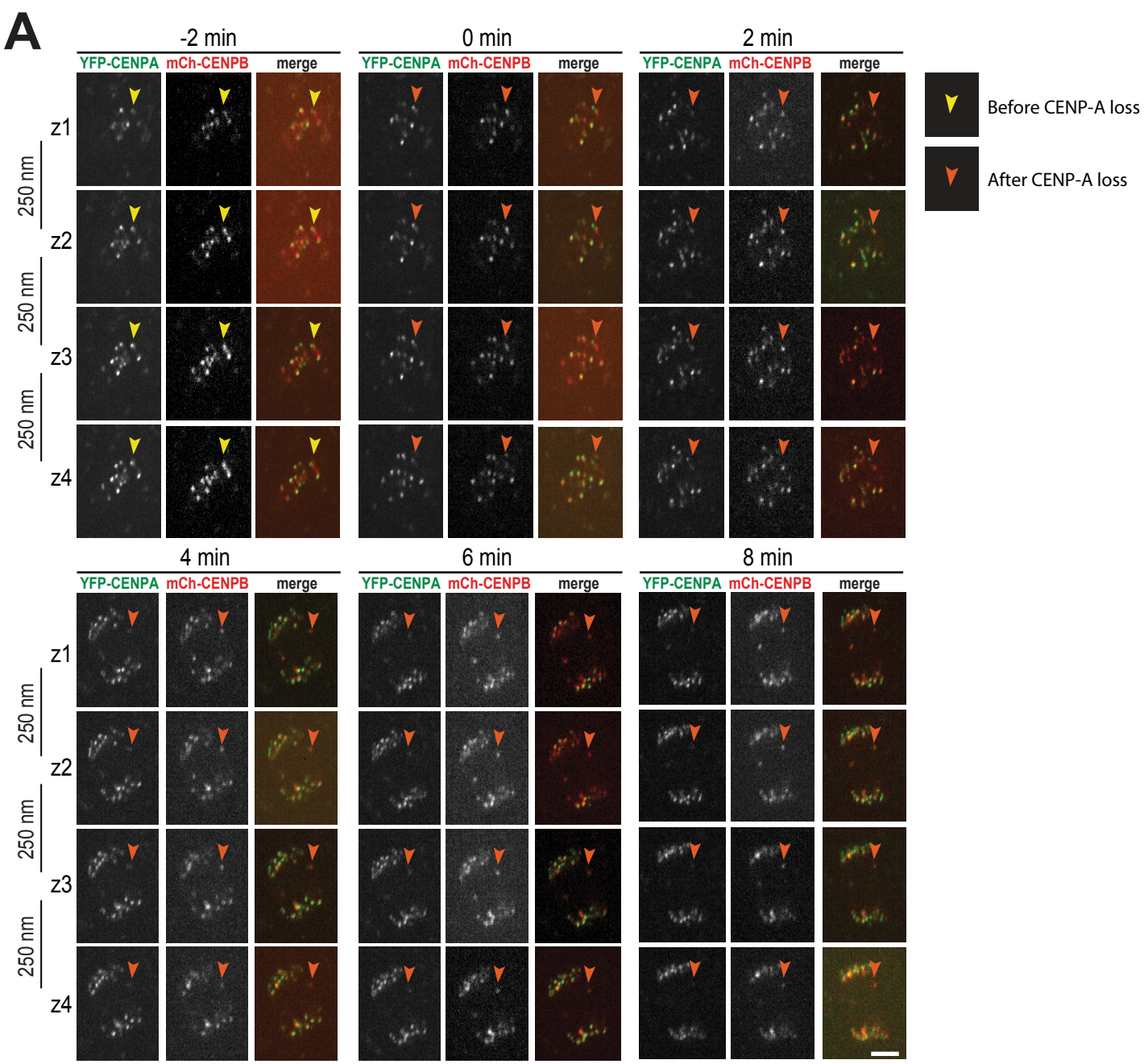
A
-2 min
0 min
2 min
4 min
6 min
8 min
YFP-CENPA
mCh-CENPB
merge
z1
z2
z3
z4
250 nm
250 nm
250 nm
Before CENP-A loss
After CENP-A loss

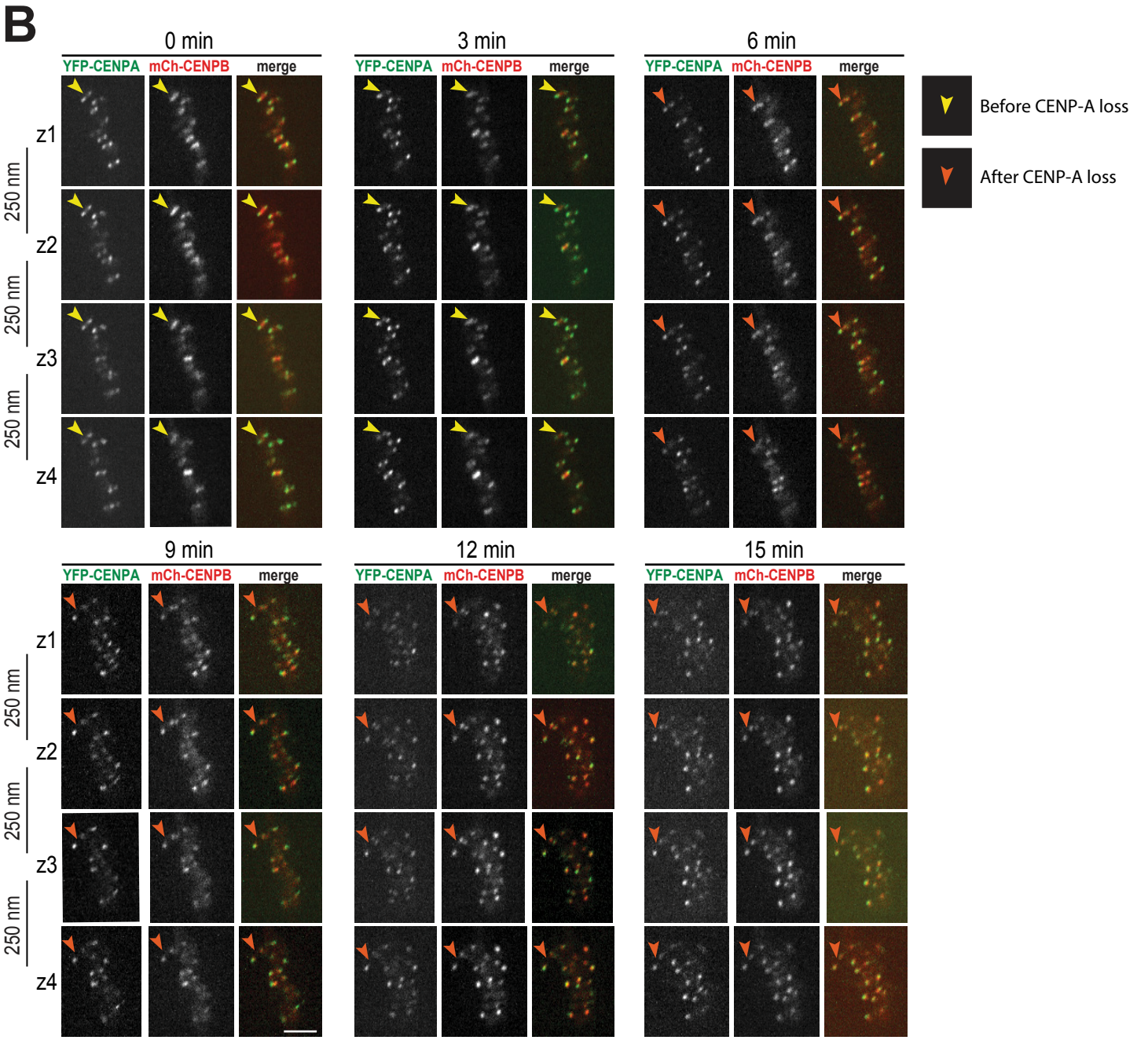

Appendix Figure S5– CENP-A loss occurs after metaphase alignment (related to Figure 4)

A Single plane images used to generate the maximum intensity projection stack in figure 4D. Arrowheads indicate kinetochore position prior to losing CENP-A (yellow) and after CENP-A loss (orange). Scale bars, 5 μm.

B Single plane images used to generate the maximum intensity projection stack in figure 4E . Arrowheads indicate kinetochore position prior to losing CENP-A (yellow) and after CENP-A loss (orange). Scale bars, 5 μm.

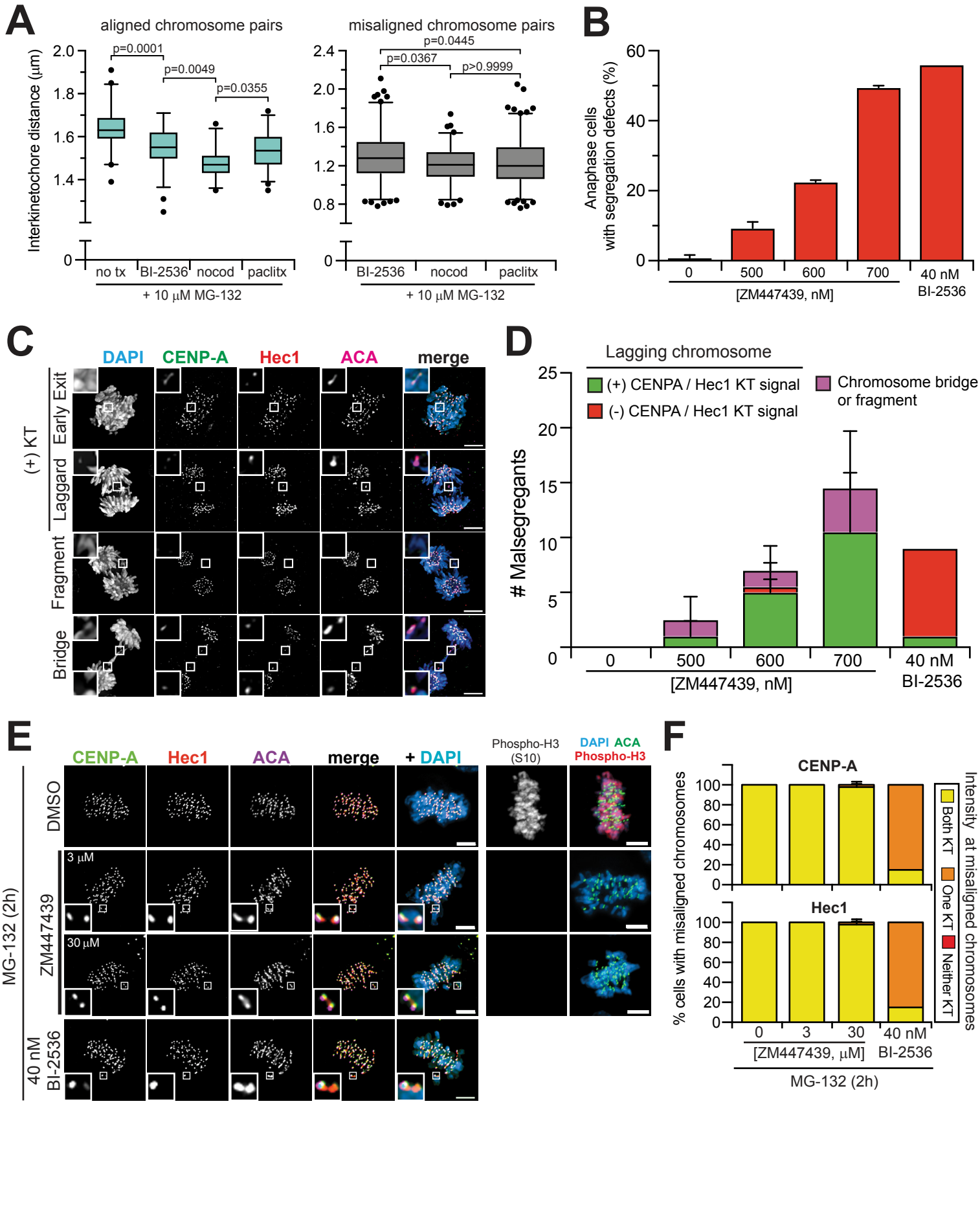
A
aligned chromosome pairs
misaligned chromosome pairs
Interkinetochore distance (μm)
p=0.0001
p=0.0049
p=0.0355
p=0.0445
p=0.0367
p>0.9999
no tx
BI-2536
nocod
paclitx
+ 10 μM MG-132
B
Anaphase cells with segregation defects (%)
[ZM447439, nM]
40 nM BI-2536
C
DAPI
CENP-A
Hec1
ACA
merge
(+) KT
Early Exit
Laggard
Fragment
Bridge
D
Lagging chromosome
(+) CENPA / Hec1 KT signal
(-) CENPA / Hec1 KT signal
Chromosome bridge or fragment
Malsegregants
E
CENP-A
Hec1
ACA
merge
+ DAPI
Phospho-H3 (S10)
DAPI ACA Phospho-H3
MG-132 (2h)
DMSO
ZM447439
3 μM
30 μM
40 nM BI-2536
F
CENP-A
Hec1
% cells with misaligned chromosomes
Intensity at misaligned chromosomes
Both KT
One KT
Neither KT
[ZM447439, μM]
40 nM BI-2536
MG-132 (2h)

Appendix Figure S6– Kinetochore disruption from Plk1 inhibition is not consistent with condensin II depletion or Aurora B kinase inhibition

A Graphs show interkinetochore distances of metaphase aligned (left) and misaligned (right) chromosome pairs after 2 h Plk1 inhibition (BI-2536), nocodazole or paclitaxel challenge. Each circle represents the average measurement of 5 aligned or 1-8 misaligned chromosome pairs/cell (n=10 cells/experiment; >= 3 independent experiments). Box represents median and interquartile range, whiskers represent 5-95 percentile. Significance determined by one-way ANOVA with Tukey correction for multiple comparisons (aligned pairs) or Kruskall-Wallis test with Dunn's correction for multiple comparisons (misaligned pairs).

B Graph shows average percentage (± SEM) anaphase cells exhibiting segregation defects after Aurora B inhibition (ZM447439) or Plk1 inhibition (BI-2536). (n= 50 cells/experiment; 2 independent experiments)

C Representative maximal intensity projection micrographs of anaphase cells from (B), indicating the major phenotypes observed: lagging chromosomes with intact kinetochores (+KT), indicated by ACA signal, chromosome fragments (DAPI+/ACA-), and chromosome bridges (DAPI signal spanning 2 ACA signals). Scale bars, 5 μm. Signals determined by qualitative observation.

D Graph shows the average number (± SD) and type of anaphase malsegregant observed in (B,C). (n= 3-20 cells/experiment; 2 independent experiments). Note, lower concentrations of ZM447439 produced fewer anaphase cells with laggards, resulting in fewer cells for analysis.

E Representative maximal-intensity projection micrographs of metaphase cells with misaligned chromosome pairs after 2h Aurora B inhibition (ZM447439) or Plk1 inhibition (BI-2536). Insets highlight distribution of CENP-A and Hec1 at misaligned kinetochore pairs, indicated by ACA. MG-132 was used to prevent mitotic cells from entering anaphase. H3(S10) phosphorylation indicates inhibition of Aurora B. Scale bars, 5 μm.

F Graphs show average percentage (± SD) metaphase cells from (E) with the indicated CENP-A or Hec1 intensity distributions at misaligned kinetochore pairs, indicated by ACA: observed at both kinetochores (yellow), observed at only one (orange), or not observed at either kinetochore (red). (n=20 cells/experiment; 2 independent experiments).

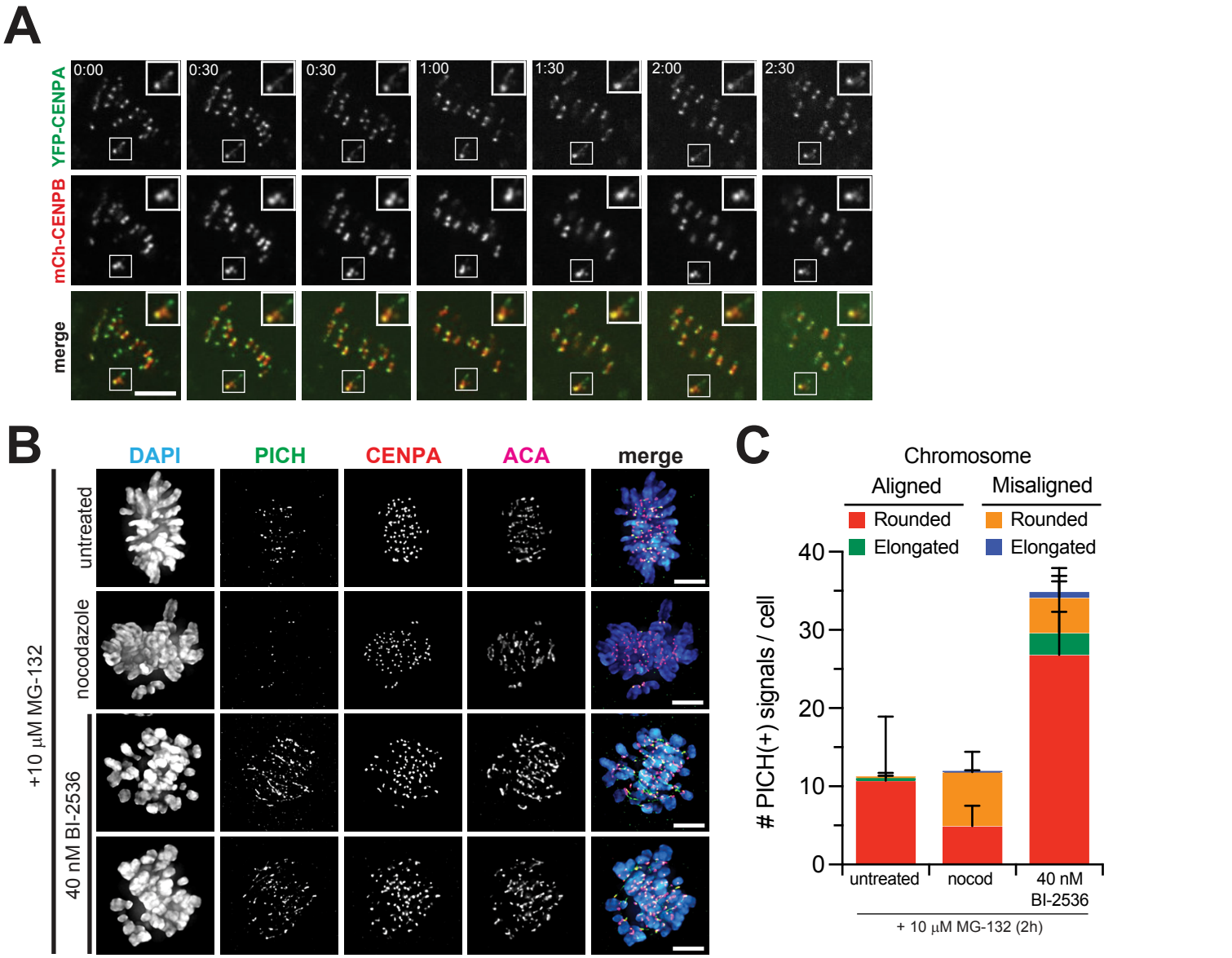

Appendix Figure S7– Reduced Plk1 activity is associated with centromere stretching and recruitment of PICH (related to Figure 5)

A Maximal-intensity projection frames from live cell fluorescence microscopy of RPE1 cells challenged with 40 nM BI-2536 to generate misaligned chromosomes. Insets highlight a misaligned chromosome pair where the YFP-CENPA signal kinetochore oscillates with respect to the intact mCh-CENPB signal at the pole-distal kinetochore. Time, in minutes:seconds from metaphase onset. Scale bar, 5 μm.

B Representative maximal-intensity projection micrographs of metaphase cells with misaligned chromosomes indicating recruitment of PICH after 2 h of no challenge, nocodazole challenge, or Plk1 inhibition (BI-2536). MG-132 was used to prevent mitotic cells from entering anaphase. Scale bars, 5 μm.

C Graph shows average number (± SD) of kinetochore-associated PICH signals observed per cell in (B). (n= 25 cells from 2 independent experiments). Data is grouped by signal shape (rounded vs. elongated) and chromosome alignment (aligned vs. misaligned).

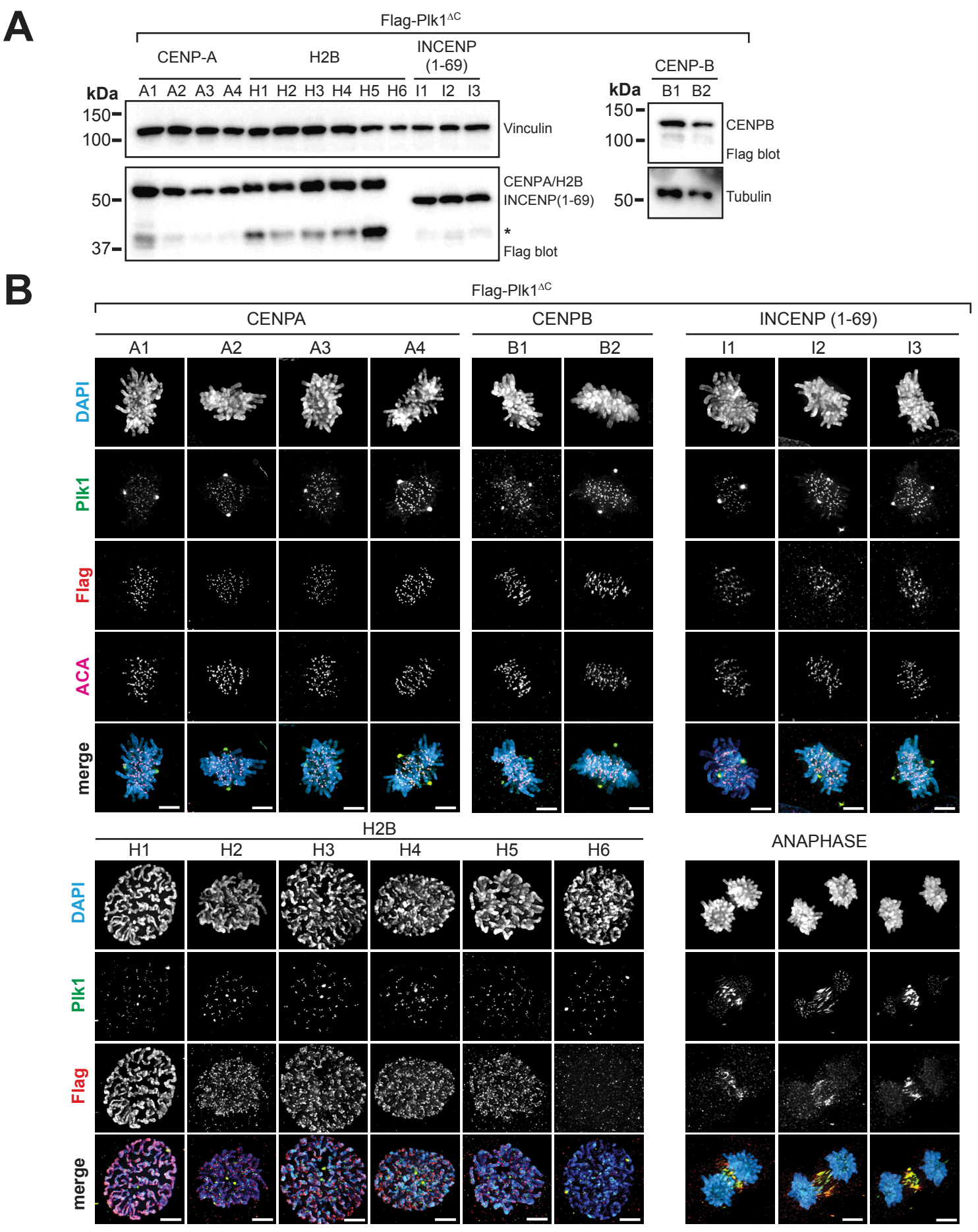
A
Flag-Plk1ΔC
CENP-A
H2B
INCENP (1-69)
CENP-B
kDa
A1 A2 A3 A4 H1 H2 H3 H4 H5 H6 I1 I2 I3
B1 B2
150
100
50
37
Vinculin
CENPA/H2B
INCENP(1-69)
*
Flag blot
CENPB
Flag blot
Tubulin
B
Flag-Plk1ΔC
CENPA
CENPB
INCENP (1-69)
A1 A2 A3 A4 B1 B2 I1 I2 I3
DAPI
Plk1
Flag
ACA
merge
H2B
H1 H2 H3 H4 H5 H6
ANAPHASE

Appendix Figure S8– Expression/localization of centromere-tethered Plk1 constructs (related to Figure 6)

A Immunoblot of protein extracts from RPE1 cell lines co-expressing EGFP-Plk1as and Flag-tagged, wildtype Plk1 kinase domain tethered to CENP-A (clones A1-A4), H2B (clones H1-H6), N-terminal INCENP (clones I1-I3), or CENP-B (clones B1-B2). Membranes probed for Flag-tagged Plk1 (Flag blot) or vinculin/tubulin (loading controls). Asterisk indicates truncation product.

B Representative maximal intensity projection micrographs of cells from (A) demonstrating localization of the indicated tethered-Plk1 products. Scale bars, 5 μm

References

1. Lera RF, Burkard ME (2012) High Mitotic Activity of Polo-like Kinase 1 Is Required for Chromosome Segregation and Genomic Integrity in Human Epithelial Cells. *J Biol Chem* **287**: 42812–42825.
2. Taylor SS, Hussein D, Wang Y, Elderkin S, Morrow CJ (2001) Kinetochore localisation and phosphorylation of the mitotic checkpoint components Bub1 and BubR1 are differentially regulated by spindle events in human cells. *J Cell Sci* **114**: 4385–4395.
3. Gascoigne KE, Takeuchi K, Suzuki A, Hori T, Fukagawa T, Cheeseman IM (2011) Induced ectopic kinetochore assembly bypasses the requirement for CENP-A nucleosomes. *Cell* **145**: 410–422.
4. Ryan SD, Britigan EMC, Zasadil LM, Witte K, Audhya A, Roopra A, Weaver BA (2012) Up-regulation of the mitotic checkpoint component Mad1 causes chromosomal instability and resistance to microtubule poisons. *Proc Natl Acad Sci* **109**: E2205–E2214.
5. Lénárt P, Petronczki M, Steegmaier M, Di Fiore B, Lipp JJ, Hoffmann M, Rettig WJ, Kraut N, Peters JM (2007) The Small-Molecule Inhibitor BI 2536 Reveals Novel Insights into Mitotic Roles of Polo-like Kinase 1. *Curr Biol* **17**: 304–315.